JOURNAL OF CATALYSIS **165,** 12–21 (1997)
ARTICLE NO. CA971443

Interaction of Chlorinated Ethylenes with Chromium Exchanged Zeolite Y: An *in Situ* FT-IR Study

Prashant S. Chintawar and Howard L. Greene[1]

Department of Chemical Engineering, The University of Akron, Akron, Ohio 44325-3906

Received February 27, 1996; revised August 15, 1996; accepted August 19, 1996

The interaction of chlorinated ethylenes (vinyl chloride, 1,1 dichloroethylene, trichloroethylene, and perchloroethylene) with the surface of chromium exchanged zeolite Y (Cr–Y) catalyst has been studied by *in situ* FT-IR spectroscopy. The adsorptions were carried out on the *in situ* oxidized Cr–Y pellet at temperatures between 25 and 300°C in a dry nitrogen stream as a means of studying possible decomposition intermediates. The adsorption at 25°C was chiefly physical in nature although some dechlorination of the molecule was evident even at this temperature. At higher temperatures, between 100 and 300°C, an oxygen attack on the adsorbed molecule led to the formation of partially and/or fully oxygenated (but still adsorbed) species. These oxygenated species, including carboxylate and carbonate, were found to contain fewer chlorine atoms than the original feed molecule. The catalytic activity for the formation of these intermediates was found to diminish with increasing chlorine content of the feed molecule. Based on these results, a reaction pathway for the progressive catalytic oxidation of chlorinated ethylenes has been proposed.

INTRODUCTION

Chlorinated ethylenes (CEs) such as vinyl chloride (VC, $H_2C{=}CHCl$), 1,1 dichloroethylene (1,1 DCE, $Cl_2C{=}CH_2$), trichloroethylene (TCE, $HClC{=}CCl_2$), and perchloroethylene (PCE, $Cl_2C{=}CCl_2$) constitute a significant fraction of the hazardous air and water pollutants. Low temperature catalytic destruction (1–4) appears to be the most popular and effective method for their remediation. However, the available literature still lacks heterogeneous thermal catalytic reaction mechanisms for their oxidation.

The destruction mechanism of these CEs, especially TCE, using other techniques has been widely studied. A large number of studies dealing with photocatalytic destruction of TCE has been reported in the literature. Pruden and Ollis (5) have reported detection of dichloroacetaldehyde ($CHCl_2CHO$) intermediate during photodecomposition of TCE over TiO_2 in aqueous solution. They proposed interaction of TCE with $OH^{\bullet}$ radicals leading to the formation of $CHCl_2CHO$ intermediate which was further mineralized to HCl and CO_2. Dibble and Raupp (6) have detected $CHCl_2CHO$ and DCE during photooxidation of TCE using *in situ* FT-IR techniques. They proposed that $CHCl_2CHO$ is then further attacked to yield complete oxidation products. Three possible reactive photocatalytic species, namely $HO_2^{\bullet}$, $HO^{\bullet}$, and O_2^{-} were suggested as responsible for the attack to produce $CHCl_2CHO$.

Kazanjian and Horell (7) have studied the radiation induced oxidation of TCE using FT-IR spectroscopy. Irradiations were carried out in a Gammacell-220, a commercial source containing about 3200 Ci of cobalt-60. The three major products identified were dichloroacetyl chloride ($CHCl_2COCl$), phosgene ($COCl_2$), and trichloroethylene oxide. A free radical mechanism was proposed to account for the observed intermediates. Similarly, Sutherland and Spinks (8) have studied radiolysis of PCE. Upon irradiation, PCE oxidized to trichloroacetyl chloride which was later found to hydrolyze to trichloroacetic acid (8).

Arnold *et al.* (9) have studied the homogeneous reaction of oxygen atoms with CEs using infrared chemiluminscence techniques. The initial step was postulated to involve the formation of an aldehyde. Reaction products observed were CO, CO_2, Cl_2, HCl, HCHO, and $COCl_2$.

More recently, Mortland and Boyd (10) studied the interaction of 1,2 DCE, TCE, and PCE with Cu(II)-smectite suspension in CCl_4 solution at reflux temperature using a combination of FT-IR, ESR, and NMR spectroscopy. The interaction was found to have resulted in dechlorination and the formation of a carbonyl group. Similarly, Song *et al.* (11) have studied the reaction of unsaturated organic halides with the gas phase vanadium clusters. The results obtained were explained in terms of three different mechanisms for the reaction of halopropene: halogen abstraction; halogen substitution followed by molecular hydrogen evaporation; and molecular addition followed by evaporation of the molecular hydrogen and hydrogen halide.

The present study was undertaken to elucidate the pathways involved in the progressive oxidation of several CEs, namely VC, 1,1 DCE, TCE, and PCE on a Cr–Y zeolite

[1] To whom correspondence should be addressed. Present address: Department of Chemical Engineering, Case Western Reserve University, Cleveland, OH 44106-7217.

0021-9517/97 $25.00

surface as a function of temperature and chlorine content of the feed, using infrared absorption spectroscopy to follow the course of reaction. The Cr–Y zeolite catalyst was chosen for this study because of its known high activity toward the complete oxidation of CEs (12). The adsorption of CEs was carried out at low (25°C) as well as high (300°C) temperatures to aid in detecting all the possible intermediates (which might not otherwise be visible at high temperature) leading to the formation of complete oxidation products.

EXPERIMENTAL

The Y zeolite (Si/Al = 2.5), containing 20 wt% alumina binder, was received from UOP in the form of 1/16″ pellets (LZY-64). Two ammonium exchanges, each lasting 3 h, were carried out on these pellets at 60°C using 2.24 M NH_4Cl solution in water. The NH_4–Y so obtained was then subjected to chromium exchange with 42.9 m*M* $CrN_3O_9 \cdot 9H_2O$ solution as a source of chromium cations, at 60°C for 72 h. The initial pH of the solution was adjusted to 4.0 by the addition of a few drops of aqueous NH_4OH. After the chromium exchange, the catalyst pellets were thoroughly washed with deionized and double distilled water, dried at 100°C and then calcined at 500°C for 12 h. This catalyst (Cr–Y) was found to contain 4.14% Cr (Phillips PV9550 X-ray fluorescence spectrometer) and had a BET (Quantasorb Jr. surface area analyzer) surface area of 430 m^2/g.

In situ FT-IR experiments were performed in a Bio-Rad model FTS-7 spectrometer at 4-cm^{-1} resolution. The spectrometer was equipped with purged bench option. The experiments were conducted in a variable temperature transmission cell (HTC-100) manufactured by Harrick Scientific. The Cr–Y catalyst samples for the reactions were made in the form of self supported pellets 13 mm in diameter using a pellet die also made by Harrick Scientific.

In a typical experiment, the catalyst pellet was calcined *in situ* at 350°C in flowing air for 3 h. The temperature of the pellet was then lowered to the desired adsorption temperature followed by 1 h evacuation to 10^{-5} Torr (1 Torr = 133.3 N m^{-2}). The FT-IR spectrum of the catalyst pellet was collected at this point and later used as a reference for subsequent adsorption spectra.

In situ adsorption of CEs on these pellets was carried out at 2000 PPM concentration in dry nitrogen (<8 PPM water) for 30 min. Preliminary adsorption experiments with dry nitrogen only (without any CE) showed no change in the zeolite spectrum indicating no contamination by the carrier gas. Rapid spectra were collected during the adsorption process and the cell was again evacuated to 10^{-5} Torr to remove the gas phase and physisorbed species. The spectrum obtained after 1 h evacuation was assigned to the chemisorbed species on the surface. Pure component gas phase spectra, used for comparison, were obtained by separately filling the empty reaction cell with 2000 PPM of CE in dry nitrogen.

In situ adsorption of CEs was carried out at three different temperatures, viz., 25, 100, and 300°C, and at a total pressure of 1 atm. The intermediate temperature of 100°C was chosen because it is higher than the normal boiling point of all the feeds except PCE. For PCE, the intermediate *in situ* adsorption experiments had to be carried out at 130°C.

RESULTS

The gas phase spectra of the four CEs in nitrogen and their interpretation are documented in Table 1. With the exception of PCE, all CEs show distinct C=C stretching bands (νC=C) in the 1575–1630-cm^{-1} region. In the gas phase, the PCE molecule has symmetry described by the point group D_{2h}. This band is therefore IR forbidden although it is visible in the Raman spectrum at 1571 cm^{-1} (13).

Adsorption of VC

Figure 1B shows the spectra obtained during VC adsorption at 25°C. The adsorption is accompanied by the detection of gas phase CO_2 as seen by a weak doublet at 2365 and

TABLE 1

Vibrational Frequencies (cm^{-1}) of Gas Phase CEs and Their Assignment

VC		1,1 DCE	
Frequency	Assignment (from (32))	Frequency	Assignment (from (13))
617	C–Cl twist	455	CCl_2 wag
709	C–Cl stretch	610	CCl_2 sym-stretch
729	C–Cl stretch	793	CCl_2 asym-stretch
897	C–Cl wag	868	CH_2 wag
941	CH_2 wag	1088	CH_2 rock
1023	CH_2 rock	1391	CH_2 scissor
1269	C–H rock	1462	CH_2 deformation
1290	C–H rock	1576	C=C stretch
1361	CH_2 deformation	1614	C=C stretch
1387	CH_2 deformation	1628	C=C stretch
1599	C=C stretch		
1605	C=C stretch		
3097	C–H stretch		
3130	C–H stretch		
TCE		PCE	
Frequency	Assignment (from (22))	Frequency	Assignment (from (13))
635	C–Cl stretch	781	CCl_2 asym-stretch
781	C–Cl stretch	916	CCl_2 sym-stretch
847	C–H bend		
941	C–Cl stretch		
1254	CH–Cl bend		
1564	C=C stretch		
1593	C=C stretch		
3098	C–H stretch		

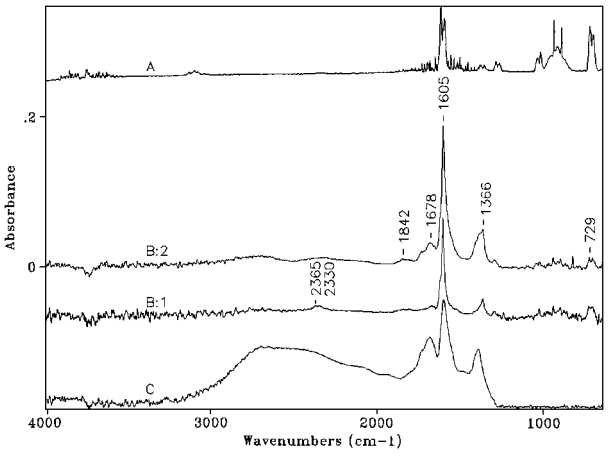

FIG. 1. FT-IR spectra of the species arising from VC adsorption on Cr–Y at 25°C. A: Gas phase VC spectrum. B, Progress of adsorption: 1, 1 min; 2, 30 min. C: Spectrum obtained after evacuation to 10^{-5} Torr.

2330 cm^{-1}. Additionally, weak bands are seen at 1678 cm^{-1} and 1842 cm^{-1}. The CO_2 doublet disappears after a few minutes of adsorption, whereas the intensity of the 1678- and 1842-cm^{-1} bands increases during the course of adsorption.

The frequency 1678 cm^{-1} is very close to the stretching frequency of the C=O bond (νC=O) of various aldehydes and ketones. For example, Finocchio *et al.* (14) have reported νC=O for methylethyl ketone at 1660 cm^{-1}, and for benzaldehyde adsorbed on $MgCr_2O_4$ catalyst at 1684 and 1653 cm^{-1}. In a separate experiment, we carried out the adsorption of $CHCl_2COCl$ on Cr–Y and detected the νC=O band at 1660 cm^{-1}. On this basis, the 1678-cm^{-1} band observed during VC adsorption in the present study is assigned to the carbonyl stretching frequency of an adsorbed aldehyde or ketone. The adsorption band observed at 1842 cm^{-1} can be ascribed to COHCl species, as the COHF molecule has been reported to show νC=O absorption at 1837 cm^{-1} (15).

Comparison of the intensities of the gas phase bands (Fig. 1A) and those observed during adsorption (Fig. 1B) indicate that C–Cl stretching bands (710 and 729 cm^{-1}) are weaker and the CH_2 deformation band (1366 cm^{-1}) significantly stronger during the adsorption than in the gas phase. However, the majority of the bands seen during the adsorption correspond to those in the gas phase VC with only minor shifts. These perturbations (changes in the relative intensity) suggest the bending of adsorbed VC molecule via the C–Cl group. A similar observation was made by Grabowski *et al.* (16) during the adsorption of C_3H_6 on the $CoO–MgO–MoO_3$ surface. The relative intensity of the CH deformation mode was substantially higher in the adsorbed phase than in the gas phase and this phenomenon was ascribed to the bending of adsorbed C_3H_6 molecule via CH_3 group.

Figure 1C shows that evacuation of the gas phase species leads to the disappearance of 729- and 710-cm^{-1} bands (νC–Cl) with the retention of the 1604-cm^{-1} (νC=C) and 1387-cm^{-1} (CH_2 deformation) bands indicating the dissociative adsorption of VC on Cr–Y surface. The retention of the νC=O band at 1678 cm^{-1} after evacuation suggests strong adsorption of aldehyde/ketone on the surface.

The spectra obtained during the adsorption of VC at 100°C are shown in Fig. 2B. These spectra are characterized by strong absorption bands at 1383 and 1607 cm^{-1}. This doublet signifies the carboxylate species of the formate type on the surface of the catalyst, the basis for which came from the adsorption of formic acid (HCOOH) on Cr–Y, as seen in Fig. 2A. These absorption bands represent asymmetric stretching (νCOO^-, asym) and symmetric stretching (νCOO^-, sym), respectively, of the carboxylate of the formate type (17). It is evident from the spectra in Fig. 2B that in addition to the carboxylate of the formate type, the moderately strong band at 1672 cm^{-1}, previously assigned to carbonyl stretching fequency of aldehye or ketone, is also observed during VC adsorption on Cr–Y at 100°C. Evacuation does not remove any of the bands suggesting that these species are strongly held on the catalyst surface (Fig. 2C).

Unlike adsorption at 100°C, which chiefly results in the formation of carboxylate of the formate type, the adsorption at 300°C leads to the formation of a mixture of noncoordinated carbonate (CO_3^{2-}) and carboxylate of the CO_2^- type as shown in Fig. 3A. While the presence of a broad band at 1576 cm^{-1} (νCOO^-, asym) along with the band at 1375 cm^{-1} (νCOO^-, sym) suggests the presence of carboxylate of the CO_2^- type on the surface (18), the absorption at 1479 cm^{-1} suggests CO_3^{2-} firmly attached to the surface (19). Evacuation does not remove the carboxylate and carbonate species, as seen in Fig. 3B.

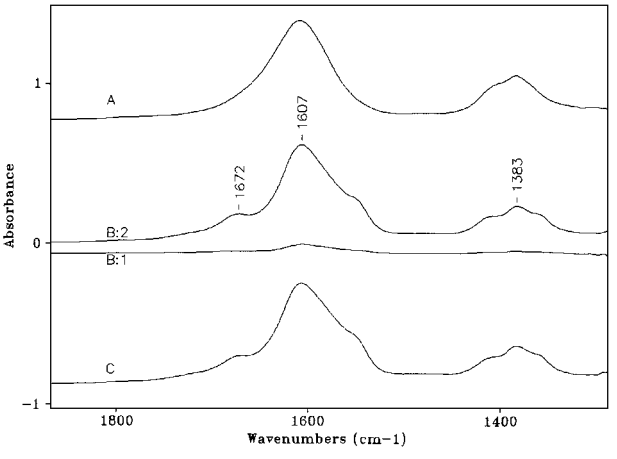

FIG. 2. FT-IR spectra of the species arising from VC adsorption on Cr–Y at 100°C. A: Bands due to carboxylate species of the formate type (Adsorption of formic acid on Cr–Y for comparison). B, Progress of adsorption: 1, 1 min; 2, 30 min. C: Spectrum obtained after evacuation to 10^{-5} Torr.

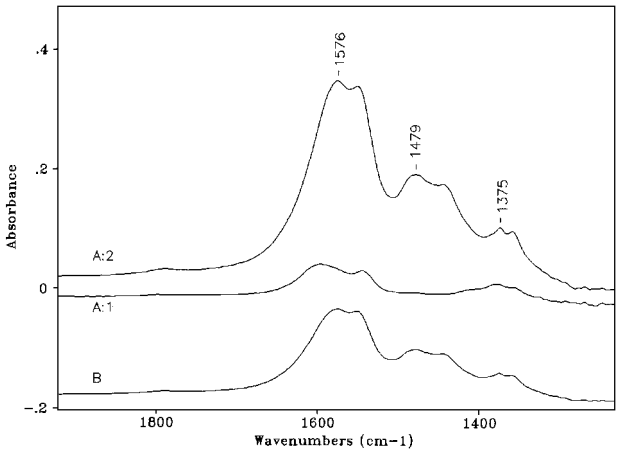

FIG. 3. FT-IR spectra of the species arising from VC adsorption on Cr–Y at 300°C. A, Progress of adsorption: 1, 1 min; 2, 30 min. B: Spectrum obtained after evacuation to 10^{-5} Torr.

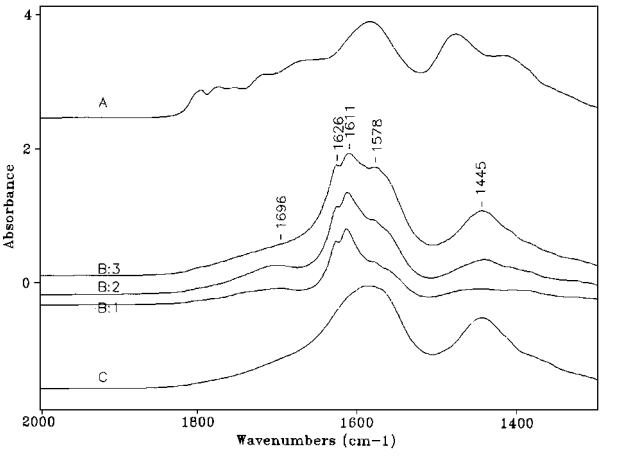

FIG. 5. FT-IR spectra of the species arising from 1,1 DCE adsorption on Cr–Y at 100°C. A: Bands due to carboxylate species of the acetate type (adsorption of acetic acid on Cr–Y for comparison). B, Progress of adsorption: 1, 1 min; 2, 7 min; 3, 30 min. C: Spectrum obtained after evacuation to 10^{-5} Torr.

Adsorption of 1,1 DCE

The 1,1 DCE adsorption at 25°C is depicted in Fig. 4B. The progress of adsorption is accompanied by an increase in the intensity of all the bands. Evacuation leads to the removal of all the bands (Fig. 4C) indicating the occurrence of only physical adsorption.

In addition to the gas phase bands at 1611 and 1626 cm^{-1} in the 1400–2000 cm^{-1} wavenumber region, as shown in Fig. 5B, 1,1 DCE adsorption at 100°C is accompanied by the formation of new bands at 1445, 1578, and 1696 cm^{-1}. The intensity of the weak band at 1696 cm^{-1} increases during the initial 7 min of adsorption and subsequently disappears. Mortland and Boyd (20) have suggested the νC=O value of ~1700 cm^{-1} for the hydrogen saturated C=O group and 1740 cm^{-1} for the chlorine saturated C=O group. Davydov (18) suggests the value of 1693 cm^{-1} for νC=O of gaseous formaldehyde (HCHO). Therefore, the band at 1696 cm^{-1} can be assigned to the gas phase HCHO. A pair of intense bands detected at 1445 and 1578 cm^{-1} (Fig. 5B) represent the carboxylate of the acetate type, which is not removed by evacuation (Fig. 5C). The basis for the assignment of the frequencies to the vibrations of carboxylate of the acetate type came from the adsorption of acetic acid (CH_3COOH) on Cr–Y as seen in Fig. 5A, where strong bands are registered at 1418, 1478, and 1587 cm^{-1}.

Interaction of 1,1 DCE with Cr–Y at 300°C is depicted in Fig. 6. Very intense bands due to carboxylate of the acetate-type species are seen at 1576 and 1443 cm^{-1} at the commencement of adsorption. Another moderate adsorption

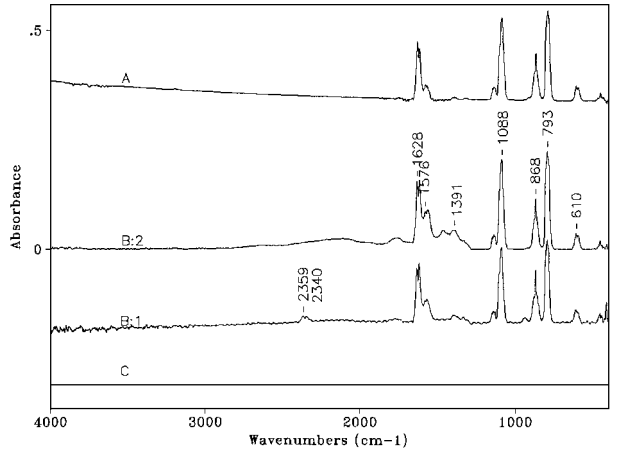

FIG. 4. FT-IR spectra of the species arising from 1,1 DCE adsorption on Cr–Y at 25°C. A: Gas phase 1,1 DCE spectrum. B, Progress of adsorption: 1, 1 min; 2, 30 min. C: Spectrum obtained after evacuation to 10^{-5} Torr.

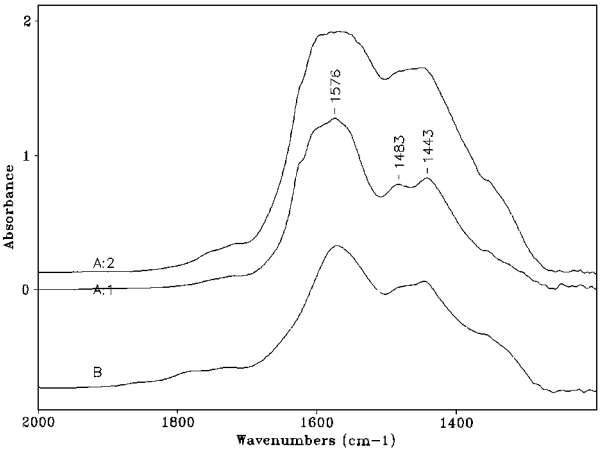

FIG. 6. FT-IR spectra of the species arising from 1,1 DCE adsorption on Cr–Y at 300°C. A, Progress of adsorption: 1, 1 min; 2, 30 min. B: Spectrum obtained after evacuation to 10^{-5} Torr.

band at 1483 cm^{-1} suggests the presence of CO_3^{2-} species, as in the case of VC. As seen from Fig. 6B, the evacuation does not remove carboxylate and carbonate species from the surface.

Adsorption of TCE

TCE adsorption at 25°C is shown in Fig. 7A. In addition to all the gas phase frequencies, a strong negative absorption is detected at 3744 cm^{-1}, which is not observed during VC and 1,1 DCE adsorption at 25°C (Figs. 1B and 4B). This frequency corresponds to silanol (Si–OH) groups on the outer surface of the crystallites; i.e., OH groups which terminate the faces of zeolite crystallites at positions where bonding in the interior would occur with adjacent tetrahedral Si or Al ions (21). A negative band at this position indicates the TCE interaction with these silanol groups.

Most of the frequencies show a negligible shift from the gas phase values with the exception of the νC–H band at 3082 cm^{-1} and the νC=C band at 1584 cm^{-1}. The νC–H band shows a net drop of 16 cm^{-1} over the gas phase frequency. This perturbation suggests that the C–H bond is involved in the adsorption process. The C=C bond shows two stretching frequencies in the gas phase at 1564 and 1593 cm^{-1} (Fig. 7A), therefore the value of 1584 cm^{-1} obtained during the adsorption cannot be interpreted properly. However, the intense nature of this band suggests the strong polarization of the C=C bond during adsorption. The evacuation leads to the removal of all the bands indicating that the adsorption is physical only, as depicted in Fig. 7C.

TCE adsorption at 100°C is shown in Fig. 8A. In addition to all the gas phase frequencies, two prominent bands are seen at 1387 and 1751 cm^{-1}. The intensity of these bands is found to increase during the course of adsorption. These bands can be assigned to the HC=O bending (δHC=O) and νC=O vibrations, respectively, of $CHCl_2CHO$ as suggested by Phillips and Raupp (22). A weak negative band is again registered at 3752 cm^{-1} indicating the interaction of TCE molecules with the Si–OH groups. However, the majority of the bands is due to gas phase TCE with negligible shifts. After 15 min of adsorption, a strong band is also seen at 1418 cm^{-1}. This band along with the band at 1584 cm^{-1} indicate the formation of carboxylate of the acetate type since the adsorption of CH_3COOH gives rise to bands at 1418, 1478, and 1587 cm^{-1} as shown in Fig. 5A. After evacuation, only the bands due to adsorbed carboxylate of the acetate type and $CHCl_2CHO$ are seen (Fig. 8B).

As seen from Fig. 9A, unlike adsorption at lower temperature, the adsorption at 300°C does not show any intermediate species like $CHCl_2CHO$. However, very intense bands

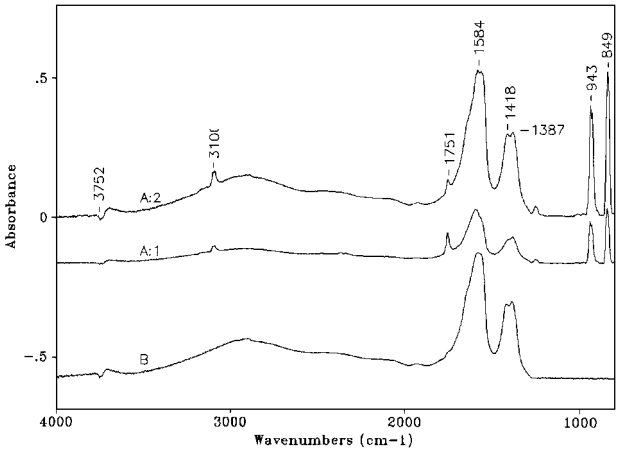

FIG. 8. FT-IR spectra of the species arising from TCE adsorption on Cr–Y at 100°C. A, Progress of adsorption: 1, 1 min; 2, 30 min. B: Spectrum obtained after evacuation to 10^{-5} Torr.

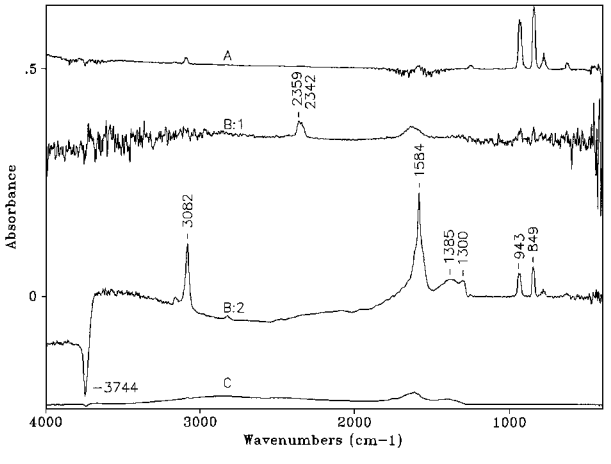

FIG. 7. FT-IR spectra of the species arising from TCE adsorption on Cr–Y at 25°C. A: Gas phase TCE spectrum. B, Progress of adsorption: 1, 1 min; 2, 30 min. C: Spectrum obtained after evacuation to 10^{-5} Torr.

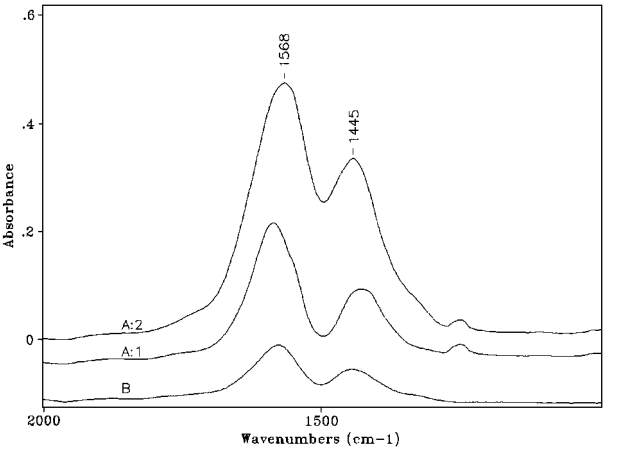

FIG. 9. FT-IR spectra of the species arising from TCE adsorption on Cr–Y at 300°C. A, Progress of adsorption: 1, 1 min; 2, 30 min. B: Spectrum obtained after evacuation to 10^{-5} Torr.

due to carboxylate of the acetate type (1568 and 1445 cm^{-1}) are seen at the commencement of adsorption. Evacuation leads to the removal of gas phase TCE and only the carboxylate species of the acetate type remains on the surface (Fig. 9B).

Adsorption of PCE

As already mentioned, the C=C stretching band is not visible in gas phase PCE due to the symmetric nature of this molecule. However, as seen from Fig. 10B, an intense vibration is registered at 1603 cm^{-1} due to νC=C during adsorption of PCE at 25°C. This band, at higher frequency than the C=C bond stretching vibration of the free molecule in the vapor phase (1571 cm^{-1}), indicates the interaction of PCE molecules with surface adsorption sites through the dissociation of one or more C–Cl bonds. As shown in Table 1, the νC=C of CEs is related to the number of chlorine atoms attached to the C=C bond. An increase in the νC=C therefore indicates a loss of one or more chlorine atoms of the PCE molecule. A similar phenomenon has been observed by Phillips and Raupp, where the νC=C of TCE was found to increase from 1597 cm^{-1} to 1609 cm^{-1} upon –Cl abstraction by coordinatively unsaturated Ti cations of the TiO_2 surface (22). In this reference, the spectrum of adsorbed TCE is matched to that of DCE.

At 25°C, the bands observed during PCE adsorption (Fig. 10B) are very similar to those found for VC. Hence, 1603 cm^{-1} corresponds to νC=C and 1354 cm^{-1} to the CH_2 deformation band of adsorbed VC (Fig. 10C) while the bands at 916 and 779 cm^{-1} can be assigned to gas phase PCE (Fig. 10A) as seen from Fig. 10. Strong silanol interaction is again observed at 3732 cm^{-1}. Strong perturbation of the C=C bond is evident from the fact that the νC=C band (invisible in the gas phase) becomes visible upon interaction with the Cr–Y surface. The adsorbed species can be easily removed by evacuation (Fig. 10D).

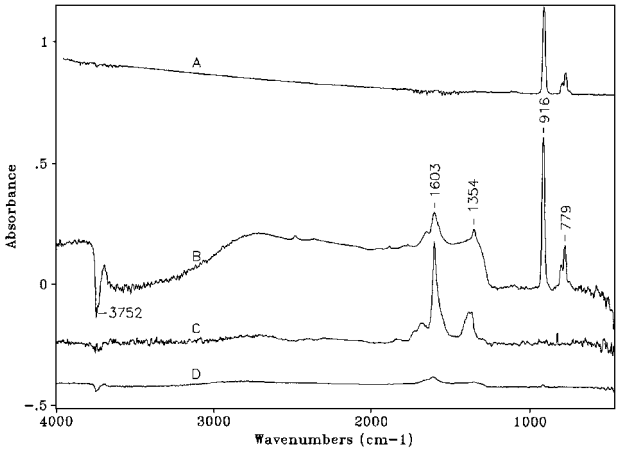

FIG. 10. FT-IR spectra of the species arising from PCE adsorption on Cr–Y at 25°C. A: Gas phase PCE spectrum; B: Spectrum obtained after 30 min adsorption of PCE; C: Spectrum of VC adsorbed on Cr–Y at 25°C (for comparison); D: Spectrum obtained after evacuation to 10^{-5} Torr.

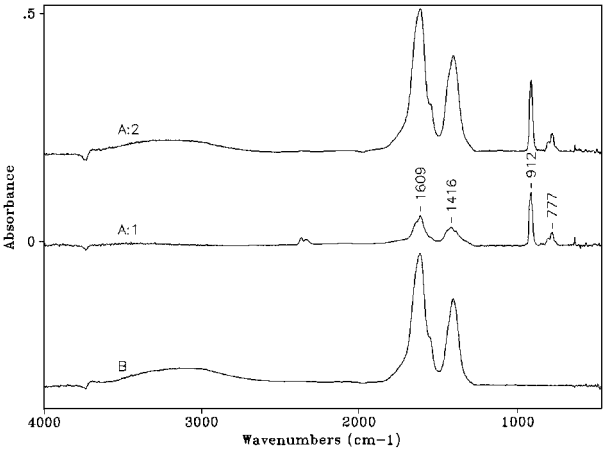

FIG. 11. FT-IR spectra of the species arising from PCE adsorption on Cr–Y at 130°C. A, Progress of adsorption: 1, 1 min; 2, 30 min. B: Spectrum obtained after evacuation to 10^{-5} Torr.

PCE adsorption at 130°C is shown in Fig. 11. Unlike with the other feeds at this temperature, there is no evidence of carbonyl formation. The strong band at 1609 cm^{-1} lies in the νC=C region and is most probably due to 1,1 DCE, since, 1,1 DCE shows the C=C stretching band at 1614 cm^{-1} (Table 1). An intense band at 1416 cm^{-1} due to the CH_2 scissor of adsorbed 1,1 DCE is also seen. The adsorption in this case, however, is irreversible since this species cannot be removed by evacuation (Fig. 11B).

PCE adsorption at 300°C is shown in Fig. 12A. As in the case of other feeds at this temperature, these spectra are characterized by strong bands due to carboxylate of the acetate type at 1591 and 1408 cm^{-1}. The adsorption is also accompanied by a weak band at 1782 cm^{-1}, suggesting the formation of small amounts of monochloroacetaldehyde

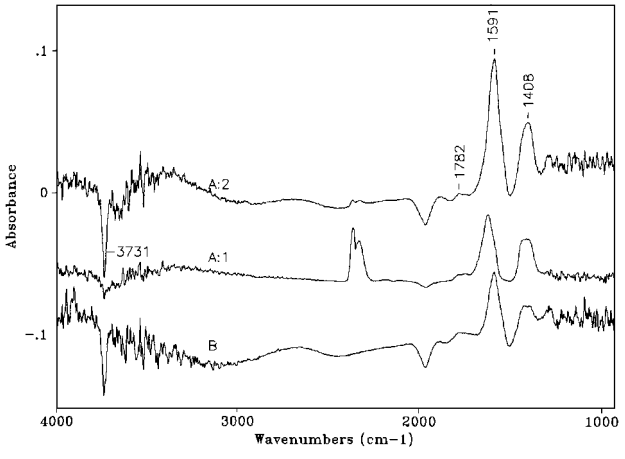

FIG. 12. FT-IR spectra of the species arising from PCE adsorption on Cr–Y at 300°C. A, Progress of adsorption: 1, 1 min; 2, 30 min. B: Spectrum obtained after evacuation to 10^{-5} Torr.

TABLE 2

Species Observed during Various Stages of Adsorption

Feed	Temperature of adsorption (°C)	Species and the bands detected
VC	25	During adsorption: gas phase CO_2, $\nu C{=}O$ of aldehyde/ketone (1678 cm^{-1}), COHCl (1842 cm^{-1}), gas phase VC After evacuation: $\nu C{=}O$ of aldehyde/ketone (1678 cm^{-1}), VC without C–Cl bond
VC	100	During adsorption: gas phase CO_2, carboxylate of the formate type (1383 and 1607 cm^{-1}), $\nu C{=}O$ of aldehyde/ketone (1672 cm^{-1}), gas phase VC After evacuation: carboxylate of the formate type (1383 and 1607 cm^{-1}), $\nu C{=}O$ of aldehyde/ketone (1672 cm^{-1})
VC	300	During adsorption: gas phase CO_2, carboxylate of the CO_2^- type (1375 and 1576 cm^{-1}), CO_3^{2-} (1479 cm^{-1}), gas phase VC After evacuation: carboxylate of the CO_2^- type (1375 and 1576 cm^{-1}), CO_3^{2-} (1479 cm^{-1})
1,1 DCE	25	During adsorption: gas phase CO_2, gas phase 1,1 DCE After evacuation: flat spectrum
1,1 DCE	100	During adsorption: gas phase CO_2, HCHO (1696 cm^{-1}), carboxylate of the acetate type (1445 and 1578 cm^{-1}), gas phase 1,1 DCE After evacuation: carboxylate to the acetate type (1445 and 1578 cm^{-1})
1,1 DCE	300	During adsorption: gas phase CO_2, carboxylate of the acetate type (1443 and 1576 cm^{-1}), CO_3^{2-} (1483 cm^{-1}), gas phase 1,1 DCE After evacuation: carboxylate of the acetate type (1443 and 1576 cm^{-1}), CO_3^{2-} (1483 cm^{-1})
TCE	25	During adsorption: gas phase CO_2, strong silanol interaction (3744 cm^{-1}), gas phase TCE After evacuation: flat spectrum
TCE	100	During adsorption: gas phase CO_2, moderate silanol interaction (3752 cm^{-1}), $CHCl_2CHO$ (1387 and 1751 cm^{-1}), gas phase TCE, carboxylate of the acetate type (1418 and 1584 cm^{-1}) (after 15 min adsorption) After evacuation: carboxylate to the acetate type (1418 and 1584 cm^{-1}), $CHCl_2CHO$ (1387 and 1751 cm^{-1})
TCE	300	During adsorption: gas phase CO_2, carboxylate of the acetate type (1445 and 1568 cm^{-1}), gas phase TCE After evacuation: carboxylate of the acetate type (1445 and 1568 cm^{-1})
PCE	25	During adsorption: gas phase CO_2, adsorbed VC, gas phase PCE After evacuation: flat spectrum
PCE	130	During adsorption: gas phase CO_2, partially dechlorinated PCE, gas phase PCE After evacuation: partially dechlorinated PCE
PCE	300	During adsorption: gas phase CO_2, carboxylate of the acetate type (1408 and 1591 cm^{-1}), CH_2ClCHO (1782 cm^{-1}), strong silanol interaction (3731 cm^{-1}), gas phase PCE After evacuation: carboxylate of the acetate type (1408 and 1591 cm^{-1})

(CH_2ClCHO) (23). Strong silanol interaction is also registered as a negative absorption at 3731 cm^{-1}. Evacuation leads to the removal of gas phase PCE; carboxylate of the acetate type, along with the negative band at silanol are the only remaining absorptions (Fig. 12B).

Table 2 summarizes the species observed during various stages of adsorption for all the feeds as a function of temperature.

DISCUSSION

Common Adsorption Features

As shown in Table 2, a common feature of all the adsorption spectra is the formation of gas phase CO_2 at the commencement of adsorption, irrespective of the feed and the temperature. This gas phase CO_2 is shown as a doublet at ~2360 and 2340 cm^{-1} in Figs. 1B, 4B, and 7B. With the progress of time of adsorption, however, the gas phase CO_2 disappears and the CEs subsequently react with the Cr–Y surface giving rise to various partial oxygenated products such as COHCl, $CHCl_2CHO$, CH_2ClCHO, HCHO, carboxylate of the type CO_2^-, formate, and acetate. Recall that adsorptions are carried out in the absence of the oxygen in the feed stream and only the initial chemisorbed oxygen is present on the catalyst surface. It is speculated that the chemisorbed oxygen (and not the gas phase oxygen) is the reactive species. This implies that the reaction pathway developed here is initially applicable to the reactions carried out in the presence of gas phase oxygen also, except that intermediates will be much more clearly visible.

Rationale for Carboxylate Assignment

As already seen, with the exception of VC, the adsorption of all CEs at 300°C leads to the formation of carboxylate of the acetate type. In addition, the adsorption of 1,1 DCE and TCE at 100°C also yields the same carboxylate. Conversely, the adsorption of VC at 100°C results in the appearance of carboxylate of the formate type and at 300°C it yields CO_3^{2-} and carboxylate of the CO_2^- type.

The assignment of a pair of bands at 1568–1591 and 1408–1444 cm^{-1} to the carboxylate of the acetate type deserves some explanation. This species is referred to as acetate because the bands are similar to those observed after the chemisorption of CH_3COOH on Cr–Y. Various researchers have previously found these bands at similar positions. Kuznetsov *et al*. (24) found the CH_3COOH adsorption bands on Cr_2O_3 at 1435 and 1555 cm^{-1} and assigned them to νCOO^- (sym) and νCOO^- (asym), respectively, of the acetate. Busca and Lorenzelli (25) detected the same bands at 1440 and 1540 cm^{-1} on αFe_2O_3 after CH_3COOH adsorption. Datka and Eischens (26) produced acetate by exposure of Pt/Al_2O_3 to C_2H_2 at 250°C and found the bands at 1460 and 1580 cm^{-1}.

The conventional coke, which is polymeric carbon, shows $\nu C{=}C$ (aromatic) at 1591 cm^{-1} along with CH_2 and CH_3 bending absorptions at 1458, 1394, and 1378 cm^{-1} (26). Since these four bands are not observed upon CE adsorption at 100 and 300°C, and the position of the bands observed is very close to that of acetate as reported by various researchers and as seen by CH_3COOH adsorption on Cr–Y, we assign them to the carboxylate of the acetate type. Table 3 shows the acetate type carboxylate stretching frequencies of these CEs only at 100 and 300°C, since no such species is formed at 25°C.

VC is excluded from Table 3 since it forms carboxylate of the CO_2^- type and not acetate. Table 3 shows that there is a distinct trend in the value of νCOO^- (sym) and νCOO^- (asym) with the chlorine content of the feed molecule. The νCOO^- (sym) decreases from 1445 cm^{-1} for 1,1 DCE to 1408 for PCE. Conversely, there is a small increase in the value of νCOO^- (asym) from 1576 cm^{-1} for 1,1 DCE to 1591 cm^{-1} for PCE. This suggests that the position of acetate type carboxylate stretching frequencies is a function of number of chlorine atoms in the feed molecule. So it is possible that this carboxylate formed is more complex than simple acetate. According to Bellamy (15), in esters, acids, and ketones the substitution of a chlorine atom on the α-carbon atom to the carbonyl group results in a small shift in the νCOO^- (asym) to a higher value. Bellamy has shown that in the vapor phase, $ClCH_2COOH$ absorbs at 1794 cm^{-1}, while CH_3COOH absorbs at 1785 cm^{-1}. Therefore, it is possible that the carboxylate formed from other CEs is not completely devoid of chlorine.

TABLE 3

FT-IR Assigned Carboxylate of the Acetate Type Stretching Frequencies of CEs at Different Temperatures

	100°C		300°C	
Feed	νCOO^- (sym) (cm^{-1})	νCOO^- (asym) (cm^{-1})	νCOO^- (sym) (cm^{-1})	νCOO^- (asym) (cm^{-1})
1,1 DCE	1445	1578	1443	1576
TCE	1418	1584	1445	1568
PCE	none	none	1408	1591

Reaction Pathway

As mentioned earlier, the adsorption of CEs was carried out at three different temperatures, viz., 25, 100 (130 for PCE), and 300°C to aid in detecting all the possible intermediates leading to the formation of complete oxidation products. The reaction scheme developed here assumes that the complete oxidation reaction of CEs proceeds through the formation of intermediates which are more easily detected at low temperatures and with less than stoichiometric oxygen present. At temperatures of 300°C and above, it is hypothesized that these intermediates are not observed because of their rapid decomposition into deeper oxidation products. Thus, the earliest intermediates would be observed at the lowest temperature and, as the temperature of adsorption is increased, these intermediates would undergo further reaction, forming deeper oxidation products.

At 25°C, only the interaction of VC with the Cr–Y surface was observed to result in the formation of a strongly adsorbed carbonyl compound. The dechlorination of the molecule was also observed since the $\nu C{=}C$ (1605 cm^{-1}) and CH_2 deformation (1366 cm^{-1}) bands were seen, whereas $\nu C{-}Cl$ was not seen in the adsorbed species. With adsorption of 1,1 DCE and TCE, no new species were detected at 25°C, indicating the occurrence of physical adsorption only. The PCE adsorption at 25°C resulted in the partial dechlorination (but no oxygen addition) of the molecule as suggested by an increase in the $C{=}C$ stretching frequency of adsorbed PCE as compared to the vapor phase molecule.

At 100°C, the VC molecule interacted further with the Cr–Y surface leading to the appearance of both an adsorbed carbonyl compound and carboxylate of the formate type. At 100°C, 1,1 DCE reacted with the surface leading to the detection of gas phase HCHO and small amounts of the carboxylate of the acetate type. Similarly, the TCE interaction resulted in the formation of CCl_2HCHO and the same carboxylate. For PCE, except for partial dechlorination, the interaction at 130°C did not lead to the formation of any oxygenated species.

At 300°C, VC adsorption led to the detection of carboxylate of the CO_2^- type and CO_3^{2-} on the Cr–Y surface.

Similarly, 1,1 DCE interaction at this temperature resulted chiefly in the formation of carboxylate of the acetate type and small amounts of CO_3^{2-}. Conversely, the TCE adsorption at 300°C led to the appearance of only carboxylate of the acetate type. Similarly, PCE interacted with the Cr–Y forming small amounts of CH_2ClCHO and carboxylate of the acetate type.

It is postulated that the first step in CE interaction with the Cr–Y surface occurs through the abstraction of one or more chlorine atoms. The chlorine abstraction is evident from the spectra obtained during VC and PCE adsorption at 25°C.

The chlorine abstraction as the first step in chlorinated hydrocarbon destruction has been proposed by other researchers also. For example, Hatje *et al.* (27) have studied the interaction of C_6H_5Cl with Pt–Y and Pd–Y surfaces. The formation of the Pt–Cl complex during the reaction was proved using XPS. Kovacs and Solymosi (28) studied the thermal and photo-induced dissociation of C_2H_5I on Pd(100) surface. The primary products of dissociation were found to be $C_2H_5^{\bullet}$ and $I^{\bullet}$. It has been shown by Phillips and Raupp (22) that TCE adsorbs dissociatively on the surface of TiO_2 at room temperature in the absence of UV radiation. The chlorine of the TCE is abstracted by a coordinatively unsaturated Ti cation, and the rest of the dichloroethylene fragment is attached to the neighboring Ti site.

At the intermediate temperature of 100°C, mainly an oxygenated species (i.e., carbonyl) is observed. This indicates that the partially dechlorinated CE molecule observed after the first step is then attacked by oxygen to yield carbonyl species, which may or may not contain chlorine. In the case of 1,1 DCE and TCE, the adsorption at 100°C led to the formation of HCHO and $CHCl_2CHO$ species, respectively. The carbonyl compounds formed are seen to contain fewer chlorine atoms than the feed molecule, thereby reinforcing the hypothesis that chlorine abstraction is the first step.

The formation of a carbonyl compound is invariably followed at 300°C by the detection of carboxylate and carbonate species. Therefore, it is postulated that in the next step(s), the carbonyl species is further attacked by the reactive oxygen forming the highly oxygenated products.

Although the exact fate of chlorine abstracted in the first step is not known, three distinct possibilities exist. The absence of νH–Cl band at 2885 cm^{-1} in all the IR spectra suggests that adsorbed or gas phase HCl is probably not formed. The formation of molecular chlorine (Cl_2), an IR invisible species, cannot be confirmed. It is hypothesized that one or more chlorine atoms abstracted in the first step, form a Cr–Cl surface complex similar to the Pt–Cl complex as suggested by Hatje *et al.* (27).

From the observed results, the following reaction scheme is proposed for the progressive catalytic oxidative decomposition of CEs on the Cr–Y surface in the absence of gas phase oxygen:

CE adsorption through chlorine abstraction
$\Rightarrow$ oxygen insertion $\Rightarrow$ carbonyl formation
$\Rightarrow$ oxygen insertion $\Rightarrow$ carboxylate formation
$\Rightarrow$ carbonate, carbon dioxide formation.

A separate investigation carried out in this laboratory has previously demonstrated that the above scheme is truly catalytic in nature. In this investigation, the stability of chromium exchanged zeolites was studied during complete oxidation of several CEs at 2400 h^{-1} space velocity and 1% CE in excess air at 500°C for 51 h. The fresh catalyst exhibited 92.5% TCE destruction efficiency which eventually dropped to 67.5% after aging. This experiment corresponded to 1270 turnovers/site, indicating a sustainable catalytic reaction.

The chlorine abstraction as the first step, followed by the scission of the remaining molecule, parallels the conclusion drawn by Finocchio *et al.* (14). In this *in situ* FT-IR study of oxidation of light hydrocarbons, it was proved that these molecules are first activated at their weakest point (i.e., the C–H bond). In the present case of CEs, and C–Cl bond is weaker than the C–H bond and hence gets activated first.

The final formation of CO_2 is not seen here, probably because of the lack of available oxygen. However, earlier work in this laboratory has shown that CO_2 is the only product when air or oxygen is passed over Cr–Y catalyst pellets initially containing adsorbed carboxylate.

This scheme is also consistent with those proposed in the literature by others (14, 29, 30). For example, Kuznetsov *et al.* (29) have studied the interaction of hydrocarbons such as C_2H_4, C_3H_6, and C_4H_8 with a Cr_2O_3 surface, known to be a good complete oxidation catalyst. The oxidation of adsorbed molecules by the oxygen of the catalyst was found to take place. Surface reactions were reported to occur with the formation of various oxygen containing species such as carboxylate and carbonate which were bound to the surface. These complexes underwent further oxidation at higher temperatures to yield complete oxidation products such as CO and CO_2.

Effect of the Chlorine Content of the Feed Molecule

The data shown in Table 2 strongly suggest a sequential reaction pathway which is not only a function of temperature but also a function of chlorine content of the CEs. Thus, VC forms significant deep oxidation products at 25 and 100°C while more highly chlorinated feeds require progressively higher temperatures to obtain the same degree of oxidation.

The diminishing catalytic activity with increasing chlorine content of the feed molecule is probably due to the chloride

poisoning of the catalyst surface. As proposed in the reaction pathway, one or more chlorine atoms are abstracted from the CE molecule during the first step of its interaction with the Cr–Y surface. Thus, with increasing chlorine content of the feed molecule, the chloride concentration of the surface is hypothesized to increase, which probably leads to the observed drop in the catalytic activity. Similar conclusions were drawn by Windawi and Wyatt (31) who studied the complete oxidation of several halogenated VOCs on a Pt-supported Al_2O_3 catalyst. Based on theoretical considerations, the authors argued that the rate limiting step in the oxidation of halogenated VOCs on this catalyst is the removal of halide from the surface.

ACKNOWLEDGMENTS

Partial funding for this research was obtained from the U.S. Environmental Protection Agency, the U.S. Air Force, and SERDP is acknowledged with appreciation. Zeolite samples were obtained from UOP. The contents of this paper should not be construed to represent EPA policy.

REFERENCES

1. Manning, M. P., Hazard. *Waste* **1**(1), 41 (1984).
2. Welden, J., and Senken, S. M., *Combust. Sci. Technol.* **47**, 229 (1986).
3. Spivey, J. J., *Ind. Eng. Chem. Res.* **26**(11), 2165 (1987).
4. Lester, G. R., "Proceedings, Air and Waste Management Association, 82nd Annual Meeting and Exposition, June 25–30, Anaheim, 1989."
5. Pruden, A. L., and Ollis, D. F., *J. Catal.* **82**, 404 (1983).
6. Dibble, L. A., and Raupp, G. B., *Environ. Sci. Technol.* **26**, 492 (1992).
7. Kazanjian, A. R., and Horell, D. R., *J. Phys. Chem.* **75**(5), 613 (1971).
8. Sutherland, J. W., and Spinks, J. W. T., *Can. J. Chem.* **37**, 79 (1959).
9. Arnold, S. J., Kimbell, G. H., and Snelling, D. R., *Can. J. Chem.* **52**, 2608 (1974).
10. Mortland, M. M., and Boyd, S. A., *Environ. Sci. Technol.* **23**, 223 (1989).
11. Song, L., Freitas, J. E., and El-Sayed, M. A., *J. Phys. Chem.* **94**, 1604 (1990).
12. Chatterjee, S., Greene, H. L., and Park, Y. J., *J. Catal.* **138**, 179 (1992).
13. Shimanouchi, T., "Tables of Molecular Vibrational Frequencies," National Bureau of Standards, Washington, 1972.
14. Finocchio, E., Busca, G., Lorenzelli, V., and Willey, R. J., *J. Catal.* **151**, 204 (1995).
15. Bellamy, L. J., *in* "The Infrared Spectra of Complex Molecules, Vol. 2," 2nd ed. Chapman and Hall, New York, 1980.
16. Grabowski, R., Efremov, A. A., Davydov, A. A., and Haber, E., *Kinet. Katal.* **22**(4), 1014 (1981).
17. Kuznetsov, V. A., Geri, S. V., Gorokhovat-skii, Y. B., and Rozhkova, E. V., *Kinet. Katal.* **18**(2), 418 (1977).
18. Davydov, A. A., *in* "Infrared Spectroscopy of Adsorbed Species on the Surface of Transition Metal Oxides," p. 39, 1st ed. Wiley, New York, 1990.
19. Kiselev, V. F., and Krylov, O. V., "Adsorption and Catalysis on Transition Metals and Their Oxides," p. 241. Springer-Verlag, New York, 1989.
20. Mortland, M. M., and Boyd, S. A., *Environ. Sci. Technol.* **23**, 223 (1989).
21. Hughes, T. R., and White, H. M., *J. Phys. Chem.* **71**(7), 2192 (1967).
22. Phillips, L. A., and Raupp, G. B., *J. Mol. Catal.* **77**, 297 (1992).
23. Bellamy, L. J., and Williams, R. L., *J. Chem. Soc.*, 3465 (1968).
24. Kuznetsov, V. A., Geri, S. V., Gorokhovat-skii, Y. B., and Rozhkova, E. V., *Kinet. Katal.* **18**(2), 418 (1977).
25. Busca, G., and Lorenzelli, V., *J. Catal.* **66**, 28 (1980).
26. Datka, J., Sabak, Z., and Eischens, R. P., *J. Catal.* **145**, 544 (1994).
27. Hatje, U., Hagelstein, M., and Förster, H., *in* "Zeolites and Related Microporous Materials: State of the Art 1994" (J. Weitkamp, H. G. Karge, H. Pfeifer, and W. Hölderich, Eds.), Vol. 84. Elsevier, Amsterdam, 1995.
28. Kovacs, I., and Solymosi, F., *J. Phys. Chem.* **97**, 11056 (1993).
29. Kuznetsov, V. A., Geri, S. V., Gorokhovat-skii, Y. B., *Kinet. Katal.* **18**(3), 710 (1977).
30. Jiang, Z., Li, C., and Xin, Q., *Cuihua Xuebao* **14**(3), 229 (1993).
31. Windawi, H., and Wyatt, M., *Platinum Metals Rev.* **37**(4), 186 (1993).
32. Gullikson, C. W., and Nielsen, J. R., *J. Mol. Spectrosc.* **1**, 158 (1957).